

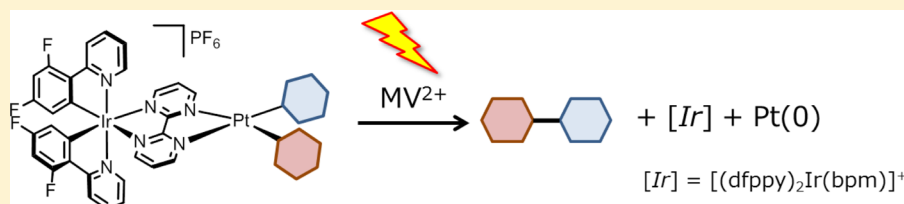
C–C Bond Forming Reductive Elimination from Diarylplatinum Complexes Driven by Visible-Light-Mediated Photoredox Reactions

Yuichiro Shiba,[†] Akiko Inagaki,^{*,‡} and Munetaka Akita^{*,†}

[†]Chemical Resources Laboratory, Tokyo Institute of Technology, R1-27, 4259 Nagatsuta, Midori-ku, Yokohama 226-8503, Japan

[‡]Department of Chemistry, Graduate School of Science and Engineering, Tokyo Metropolitan University, Minami-Osawa 1-1, Hachioji, Tokyo 192-0397, Japan

S Supporting Information



ABSTRACT: A series of dinuclear Pt(II) bis-aryl complexes with visible-light-absorbing Ir(III)–cyclometalate units were synthesized, and their molecular structure and photophysical and electrochemical properties were investigated. The dinuclear complexes underwent reductive elimination upon visible-light irradiation at ambient temperature to afford the corresponding biaryls. The photoredox process at the Ir center induces the oxidation of the Pt(II)–Ar₂ center to [Pt–Ar₂](III) to accelerate reductive elimination.

INTRODUCTION

Recently, direct C–H functionalization has become a powerful tool in organic synthesis. Of all the various transition metals, Pd complexes are particularly useful, and a vast number of their reactions have been reported to date.¹ However, examples of catalytic transformation reactions with metals from the same group as Pd are very limited,² although Pt complexes possess high potential for oxidative addition of various nonactivated C–H bonds.³ One of the reasons for this is the reluctance of Pt complexes to undergo reductive elimination. Thus, it is important to control and accelerate the reductive elimination of various Pt complexes to increase the variety of C–H functionalization.

Reductive elimination is an important elementary reaction that eliminates a product from a metal center to form a new bond. The substrate scope and catalytic activity of the coupling reactions in various molecular transformations are largely due to this reductive elimination step and the preceding oxidative addition step. For compounds of group 10 metals, the reaction rate of the reductive elimination step follows the order Ni > Pd > Pt.⁴ Important factors that can accelerate this step are (a) the steric bulk⁵ and electronic effects⁶ of the ancillary ligands, (b) the electronic effects of ligands on the metal center,⁷ and (c) the oxidation state of the metal center. Thus, fine tuning of the ancillary ligand is necessary for the construction of high-performance catalytic reaction systems. If it were possible to control one of these factors through external stimuli, it would be possible to control the reaction itself. Recently, Bergman and Tilley have reported the drastic acceleration of reductive elimination from a diarylplatinum complex by using tris(pentafluorophenyl)borane as a remote Lewis acid trigger.⁸

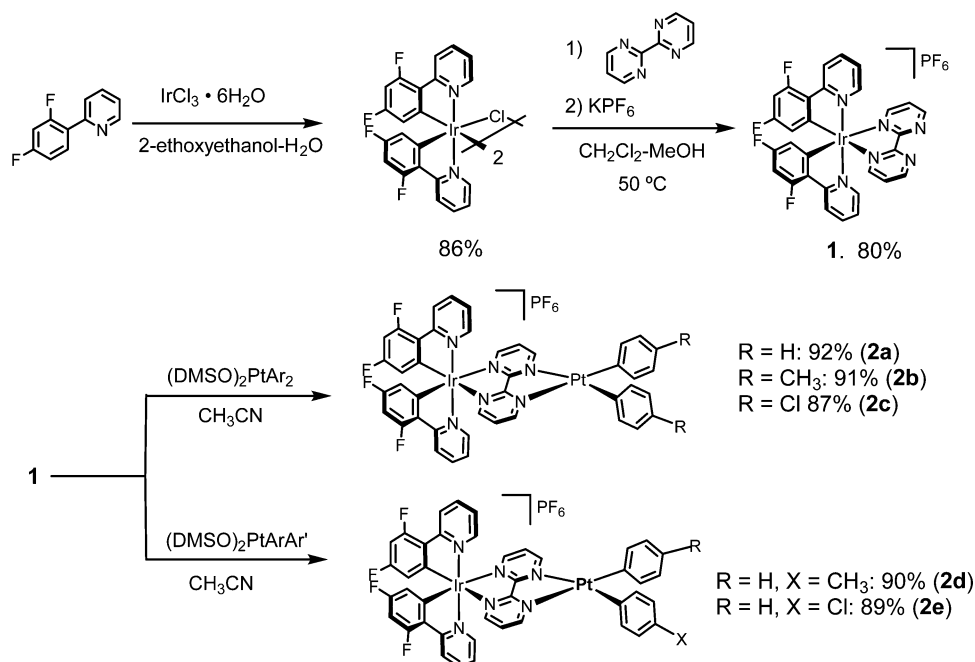
In this report, formation of the Pt(IV) intermediate contributed to the acceleration. Light is an innocent, clean, switchable, and easily controlled external stimulus for organic systems, in contrast to chemical and thermal triggers. If the reactivity can be tuned with light as an external stimulus,⁹ it would be of great advantage to realize various catalytic transformations.

The complex tris(bipyridyl)ruthenium(II) ([Ru(bpy)₃]²⁺) has been well studied because of its outstanding photochemical properties such as the generation of a long-lived triplet excited state upon visible-light irradiation through the metal-to-ligand charge-transfer (MLCT) process.¹⁰ Additionally, in the presence of an electron donor or electron acceptor, the excited species ([Ru(bpy)₃]^{2+*}) can accept or donate one electron to induce redox processes. In other words, the photoexcited species of the Ru complex can act as a strong one-electron oxidizing or reducing agent. Cyclometalated iridium(III) complexes bearing phenylpyridine ligands act as one-electron photoredox agents, similar to the case for the tris(bipyridyl)ruthenium(II) complex.¹¹ Because of its higher photoredox potential in comparison to that of the corresponding tris(bipyridyl)ruthenium(II) complex,¹² cyclometalated iridium(III) complexes are frequently used as photoredox catalysts in various organic transformations.¹³

We have been investigating visible-light-driven catalytic transformations of various organic molecules using Ru–Pd dinuclear complexes composed of a tris(bipyridyl)ruthenium derivative and a Pd–alkyl moiety.¹⁴ In these reactions, active excited species were generated via an intramolecular energy

Received: October 29, 2014

Scheme 1. Syntheses of Ir–Pt Dinuclear Complexes



transfer;^{14a} thus, the dinuclear motif of the Ru–Pd complex was essential for the reactions. We have also demonstrated the effectiveness of a facile intramolecular electron transfer for the dinuclear Ru system to generate high-oxidation-state Ru(IV)–oxo species in the photoredox-mediated catalytic oxygenation of sulfides.¹⁵ On the basis of this background, we started to investigate the reductive elimination of dinuclear Ir–Pt bis-aryl complexes to take advantage of the intramolecular electron transfer process.

Here, to control the reductive elimination of metal complexes by using light as an external stimulus, we introduced a photoredox Ir(III)–cyclometalate moiety into the diarylplatinum complexes, to develop visible-light-driven reductive elimination.

RESULTS AND DISCUSSION

Syntheses and Structures. *Syntheses.* The synthetic scheme for the dinuclear Ir–Pt bis-aryl complexes is summarized in Scheme 1. We chose the cyclometalated Ir complex **1** with 2-(2,4-difluorophenyl)pyridine (dfppy) as the light-absorbing unit, since **1** possessed better photophysical properties, such as long excited-state lifetime, among the related Ir(III) compounds with 2,2'-bipyrimidine (bpm) as the ligand.¹⁶ It is also known that photoexcited species of cyclometalated Ir complexes having electron-withdrawing fluorinated phenylpyridine ligands possess redox potentials higher than those of the corresponding cyclometalated Ir complexes with unsubstituted phenylpyridine ligands and other Ru(II) diimine complexes.^{13c}

The light-absorbing unit **1** was synthesized by treating the dichloride dimer $[(\text{dfppy})_2\text{IrCl}]_2$ with bpm, followed by the addition of KPF_6 to isolate the product as a PF_6 salt. Dinuclear Ir–Pt complexes **2a–c** were synthesized through the reaction of **1** with the diarylplatinum precursors $(\text{DMSO})_2\text{PtAr}_2$ ($\text{Ar} = \text{phenyl}, 4\text{-methylphenyl}, 4\text{-chlorophenyl}$)¹⁷ in acetonitrile ($50\text{ }^\circ\text{C}$, 2 h). Similarly, on reaction with Pt precursors that have different aryl groups ($\text{Ar} \neq \text{Ar}'$),¹⁸ the corresponding unsymmetrical

compounds **2d,e** were formed in a straightforward manner. All of the dinuclear Ir–Pt complexes have been unambiguously characterized on the basis of ^1H and ^{13}C NMR and MS spectroscopic data.

Structures. The molecular structures of **2a,b** were determined through single-crystal X-ray diffraction. ORTEP diagrams of the two compounds with anions omitted are shown in Figure 1, and crystallographic data and selected structural parameters are shown in Table 1 and Table S1 (Supporting Information), respectively.

Ir–N and Ir–C bond lengths are within the normal ranges reported for various $\text{Ir}(\text{ppy})_3$ complexes.¹⁹ Although the pyrimidine rings in **1** were slightly twisted ($\angle\text{N5–C26–C27–N6} = -13.2^\circ$) probably due to electronic repulsion between the N5 and N6 lone pairs,²⁰ the corresponding angles became much smaller after coordination to the Pt unit ($\angle\text{N5–C26–C27–N6} = 1.1(12)^\circ$ in **2a**, $\angle\text{N5–C26–C27–N6} = -1.9(14)^\circ$ in **2b**; Table 1). Turning our attention to the Pt centers, we found that the Pt–N and Pt–C bond lengths were very similar to those in the mononuclear Pt complex $(\text{bpy})\text{PtMe}_2$ (Table 1).²¹

Photophysical and Electrochemical Properties. *Electronic Absorption and Emission Data.* All UV–vis absorption spectra have been measured in DMF solutions at ambient temperature (Figure 2), and data are collected in Table 2. Emission spectra were measured by 365 nm excitation, and quantum yields were calculated relative to the value of $[\text{Ru}(\text{bpy})_3]\text{Cl}_2$ in acetonitrile ($\Phi = 0.062$).²²

In the UV–vis absorption spectra, a broad and intense absorption band is observed in the range 200–300 nm, which can be assigned to ligand-centered (LC) $^1\pi\text{--}\pi^*$ transitions of the cyclometalated and ancillary ligands. On the other hand, broad absorption bands at longer wavelengths (310–410 nm) are attributed to charge transfer transitions with mixed metal to ligand and ligand to ligand charge transfer (MLCT/LLCT) character.²³ On comparison of the spectra of the mononuclear Ir and dinuclear Ir–Pt complexes, the introduction of the Pt unit apparently gives rise to the characteristic band (around 520 nm) in the lower energy region. It is known that the

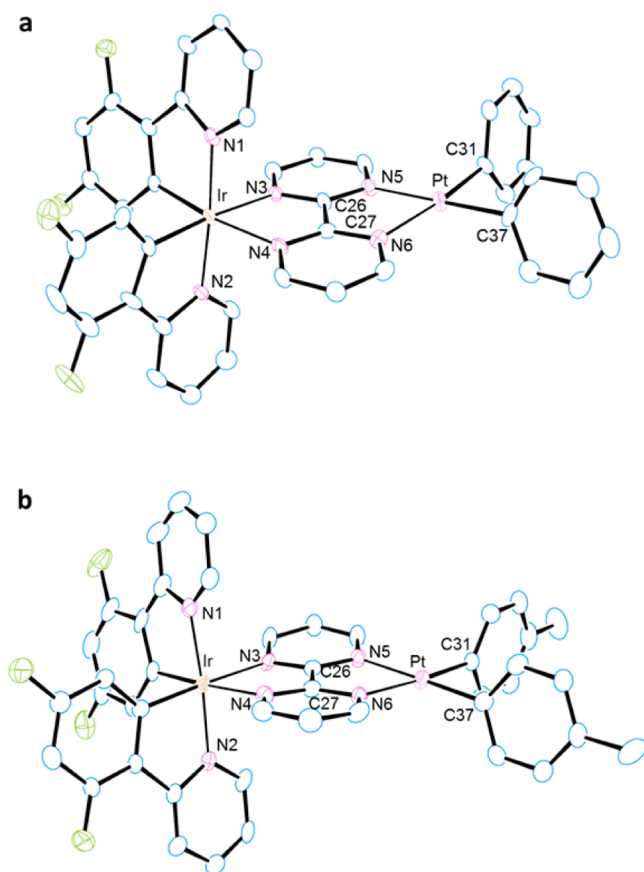


Figure 1. Crystal structures of (a) **2a** and (b) **2b** with anions omitted.

Table 1. Structural Parameters for **1** and **2a,b**

	1 ²⁰	2a	2b	(bpy) PtMes ₂ ²¹
Bond Lengths (Å)				
Ir–C11	2.024(8)	1.997(8)	2.021(11)	
Ir–C22	2.035(7)	2.013(8)	2.025(9)	
Ir–N1	2.045(7)	2.060(7)	2.034(10)	
Ir–N2	2.053(7)	2.045(7)	2.047(9)	
Ir–N3	2.174(5)	2.133(6)	2.138(8)	
Ir–N4	2.133(7)	2.149(7)	2.164(9)	
Pt–N5		2.110(7)	2.089(9)	2.095(8)
Pt–N6		2.135(7)	2.128(8)	2.090(8)
Pt–C31		2.003(8)	2.001(11)	2.016(10)
Pt–C37		2.051(9)	1.991(11)	2.032(9)
Bond Angles (deg)				
C11–Ir–N1	79.8(3)	80.5(3)	79.3(5)	
C22–Ir–N2	80.1(3)	80.2(3)	81.1(4)	
N3–Ir–N4	76.4(2)	78.1(3)	77.7(3)	
N2–Ir–N4	83.8(3)	88.7(3)	85.6(3)	
Torsion Angles (deg)				
N5–C26–C27–N6	–13.2(11)	1.1(12)	–1.9(14)	

diarylplatinum complex (bpy)PtPh₂ shows a broad mixed metal ligand to ligand charge transfer (MMLLCT; $d_{Pt-C} \rightarrow \pi^*_{bpy}$) band around 450 nm.²⁴ The solutions of **1** and (bpy)PtPh₂ are pale yellow, whereas the solution of **2a** is black owing to the red-shifted and extremely broad MMLLCT band of 460–660 nm. The spectra of the para-substituted Ir–Pt dinuclear complexes **2b,c** and unsymmetrical bis-aryl complexes **2d,e**

were almost identical with that of **2a**. Complex **1** displays an intense emission with a maximum at 608 nm. In comparison with mononuclear complex **1**, all of the dinuclear Ir–Pt complexes display weak emissions due to energy transfer to the Pt center or by partial self-absorption.

CV Spectral Data. The electrochemical behaviors of **1** and **2a–e** were investigated by cyclic voltammetry (CV) in acetonitrile (Figure 3), and the data are summarized in Table 3. The CV chart of **1** displays two reversible waves in the cathodic region at –1.36 and –2.04 V and one quasi-reversible wave in the anodic region at +1.26 V. The first two reversible waves are attributed to one-electron processes of the bipyrimidine (bpm/bpm^{•-}) and cyclometalated (dFppy/dFppy^{•-}) ligands, respectively. The quasi-reversible wave is attributed to the oxidation process of the highest occupied molecular orbital, which is dominated by Ir–C σ bond character (designated as Ir–C/Ir/C^{•+}).^{25,26} The CV charts of dinuclear complexes **2a–e** exhibit additional irreversible peaks at ~ 1.0 V, which can be attributed to the [Pt–Ar]^{II}/[Pt–Ar]^{III} oxidation process (vide infra). There have not been many platinum(III) derivatives characterized until now; most of them are binuclear species with a Pt–Pt bond. However, a few monomeric Pt(III) complexes have been structurally and electrochemically described and authenticated.^{27,24} Among them, a reversible one-electron redox couple (Pt(II)/Pt(III)) of a platinum complex, (bpm)-PtMes₂ (Mes = mesityl), was shown to be 0.45 V vs Fc/Fc⁺, because of effective axial protection by two mesityl groups. A highly irreversible wave in anodic oxidation as a result of Pt^{III} formation was reported in the α -diimine LPtPh₂ complexes in the range 0.64–0.96 V, similar to the case for the Ir–Pt complexes.²⁸

With respect to the aryl substituent on the Pt center, the slight peak shifts of **2b,c** in comparison to that of **2a** are due to the electronic nature of the para substituents of the aryl ligand. The other three peaks shift to the anodic side by 0.3–0.6 V because the electron density decreased as a result of introduction of the Pt unit. The redox potential of the Pt–Ar moiety is much lower than those of the corresponding Ir^{III/IV} processes, indicating that Ir(IV) species resulting from the photochemical processes may bring about the subsequent oxidation of the [Pt–Ar]^{II} moiety to [Pt–Ar]^{III}.

In order to gain additional information on the electrochemical behavior, we have conducted DFT calculations for complexes **2–c** and the dicationic form of **2a** ([**2a**]⁺). The following basis sets were used in the ground-state geometry optimization using Gaussian 09²⁹ program packages: LanL2DZ for Ir and Pt, 6-31G+ for N and C atoms coordinated to Pt and Ir, 6-31G for Cl in complex **2c**, and 3-21G for the other C, F, H, and N atoms. The Ir–N, Ir–C, Pt–N, and Pt–C bond lengths and the chelate angles between Ir and ppy, Ir and bpm, and Pt and bpm ligands of the optimized structures of **2a–c** reproduced the experimental results well within 1–2% differences (Figure S6 in the Supporting Information).

The highest occupied molecular orbital (HOMO) of **2a** is depicted in Figure 4, and the other corresponding other molecular orbitals of **2a–c** are given in the Supporting Information.³⁰ For complexes **2a–c**, the HOMO consists of conjugated platinum d orbitals and π orbitals equally delocalized on two aryl ligands. When Mulliken charges were compared between [**2a**]⁺ (dication) and **2a** (monocation), the corresponding values of the platinum center and the sum of the 12 carbon atoms of the phenyl groups were considerably increased in [**2a**]⁺, while the Ir center and other atoms did not show

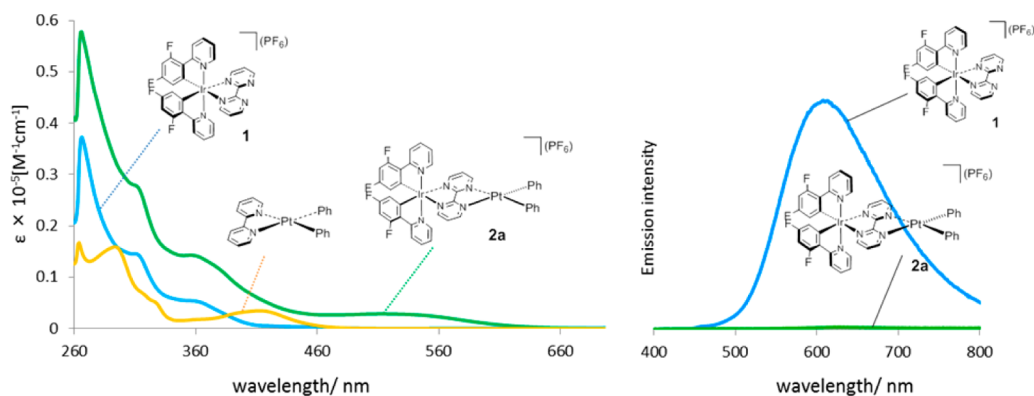


Figure 2. UV-vis absorption and emission (λ_{ex} 365 nm) spectra.

Table 2. Absorption and Emission Spectroscopic Data of Ir-Pt Complexes^a

complex	absorption, nm (ϵ , 10^{-5} M ⁻¹ cm ⁻¹)	emission	
		λ_{max} nm ^b	Φ_{rel} ^c
1	266, 315, 365	608	0.032
(bpy) PtPh ₂	264 (0.167), 294 (0.159), 413 (0.034)	546 ^d	0.0011 ^d
2a	267 (0.569), 314 (0.269), 354 (0.143), 514 (0.028)	604	0.0019
2b	264 (0.496), 312 (0.220), 357 (0.115), 512 (0.023)	601	0.0011
2c	264 (0.517), 312 (0.226), 360 (0.118), 504 (0.027)	603	0.0013
2d	264 (0.519), 312 (0.218), 356 (0.115), 515 (0.022)	601	0.0011
2e	265 (0.512), 315 (0.220), 362 (0.119), 508 (0.027)	601	0.0015

^aMeasured in DMF. ^b λ_{ex} 365 nm. ^cQuantum yield relative to TB in MeCN ($\Phi = 0.062$). ^d λ_{irr} 532 nm, measured in THF, reported by Zális et al.²⁴

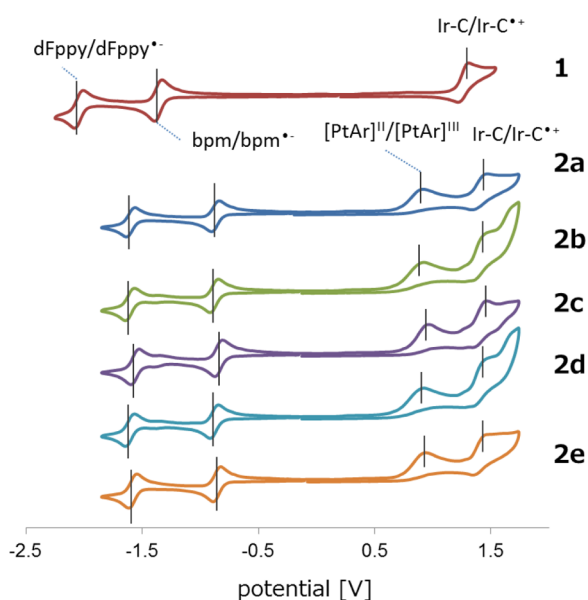


Figure 3. Cyclic voltammograms of Ir-Pt complexes.

significant changes (Table S6 in the Supporting Information). Additionally, Mulliken spin density is localized over the Pt atom (0.3066) and the carbon atoms of the phenyl ligands. These results show that the first oxidation peak in CV spectra is not a

purely metal based but is a redox process of the Pt-Ar hybrid orbitals with metal participation, which can be described as $[\text{Pt-Ar}]^{\text{II}}/[\text{Pt-Ar}]^{\text{III}}$.

Photolysis of Ir-Pt Complexes. All light-driven reductive elimination reactions were performed in 5 mm i.d. Pyrex NMR tubes containing a mixture of 0.01 mmol of Ir-Pt complex and 10 equiv of electron acceptor dissolved in 0.45 mL of deuterated solvent. The tube was placed in a beaker filled with water (thermal trap), and the sample was irradiated by a Xe lamp with an L-42 cutoff filter or an LED lamp (λ 425 nm, 3 W). For the dark reactions, the sample tubes were wrapped with aluminum foil and irradiated.

Results of visible-light-driven reductive eliminations under various conditions are summarized in Table 4. Under these conditions, LED lamp irradiation (λ 425 nm) led to a much higher yield of the biaryl (entry 1 vs 2). When other solvents (entries 2–5) and acceptors (entries 5–8) were tested, the reaction in DMSO-*d*₆ with methylviologen (MV^{2+}) as an electron acceptor led to the highest yields. Consequently, the conditions in entry 8 were selected for the following reactions. When either acceptor or light was not present, the reactivity decreased drastically (entries 9 and 10). Upon irradiation of **2a** under the selected conditions, the ¹H NMR signals of biphenyl gradually grew, while in the dark, only the signals of mononuclear Ir complex **1** were observed because of decomposition (Figure S2 in the Supporting Information).

Reductive elimination of the other Ir-Pt dinuclear symmetrical and unsymmetrical bis-aryl complexes **2b–e** was examined under the selected conditions, and the results are summarized in Table 5. All of the complexes formed the corresponding biaryls together with a mononuclear Ir complex ($[(\text{dfppy})_2\text{Ir}(\text{bpm})]^+$) and a Pt(0) mirror. If the substituents (X, Y) on the aryl ligands were either H or CH₃, the biaryl yield became 80% after 36 h of irradiation (entries 1, 2, and 4). On the other hand, the yield gradually lowered according to the number of electron-withdrawing groups introduced into the X and/or Y position (entries 3 and 5). The trend was similar to the reductive elimination of various Pd(II) complexes with diphosphine ligands.⁷ Of note, biaryl formed in the reaction of an unsymmetrical bis-aryl complex (**2e**) did not contain biphenyl (X, Y = H) or 4,4'-dichlorobiphenyl (X, Y = Cl) (Figure S4 in the Supporting Information). The result rules out the intermolecular aryl transfer process in the reaction. When a 1/1 mixture of mononuclear Ir complex **1** and Pt(bpy)(*p*-tol)₂ ((2,2'-bipyridyl)bis(4-methylphenyl)platinum) was irradiated under the same conditions, only a small amount of 4,4'-dimethylbiphenyl (entry 6) was formed (7%), and MV^{2+} was

Table 3. Electrochemical Data of Ir–Pt Complexes^a

complex	reduction		oxidation	
	dFppy/dFppy ^{•-}	bpm/bpm ^{•-}	[Pt–Ar] ^{II} /[Pt–Ar] ^{III}	Ir–C/Ir–C ^{•+}
1	–2.04	–1.36		1.26
2a	–1.50	–0.77	1.02 (irr)	1.57
2b	–1.50	–0.77	0.91 (irr)	1.63
2c	–1.45	–0.73	1.08 (irr)	1.57
2d	–1.50	–0.77	1.03 (irr)	1.59
2e	–1.47	–0.75	1.05 (irr)	1.57

^aMeasurements were carried out in CH₃CN with 0.1 M [Bu₄N]BF₄; values are given in units of V vs E(Fc/Fc⁺). irr stands for an irreversible redox wave.

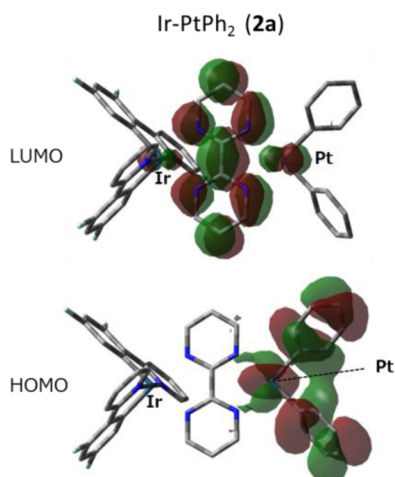


Figure 4. Frontier orbitals of 2a.

quickly consumed through the photoredox reaction with 1. The result clearly indicates the importance of the dinuclear Ir–Pt motif in the reductive elimination.

From the above results, it is clear that the reductive elimination from the diarylplatinum(II) complexes giving biaryls was driven by the photoredox process at the Ir site. All of the

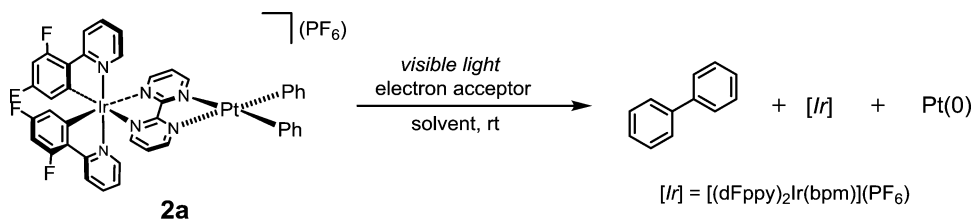
Table 5. Reductive Elimination of Biaryls^a

complex	X	Y	time (h)	yield (%) ^b
1 2a	H	H	36	88
2 2b	CH ₃	CH ₃	36	83
3 2c	Cl	Cl	72	55
4 2d	H	CH ₃	36	81
5 2e	H	Cl	48	61
6 1 + (bpy)Pt(tol) ₂	CH ₃	CH ₃	36	7

^aGeneral conditions: complex (0.01 mmol), MV²⁺ (0.10 mmol), in DMSO-*d*₆, irradiation with 3 W blue LED lamp (425 ± 15 nm) at a distance of 5 cm away from the light source. ^bDetermined by ¹H NMR using 1,4-dimethoxybenzene as an internal standard.

reactions proceeded under remarkably mild conditions for diarylplatinum reductive elimination, which normally requires heating to nearly 100 °C in bis-phosphine systems.⁶

In all of the reactions, the presence of an electron acceptor and visible light is necessary to accelerate the reductive elimination (Table 4, entries 8–10). In order to confirm that the acceleration is based on an oxidative quenching operated at the

Table 4. Visible-Light-Mediated Reductive Elimination of Biphenyl^a

entry	solvent	acceptor (A)	light source	time (h)	yield (%) ^b
1	CD ₃ CN	BQ	xenon lamp	72	10 ^c
2	CD ₃ CN	BQ	blue LED	72	56 ^c
3	CD ₃ NO ₂	BQ	blue LED	72	12
4	acetone- <i>d</i> ₆	BQ	blue LED	72	43
5	DMSO- <i>d</i> ₆	BQ	blue LED	60	76
6	DMSO- <i>d</i> ₆	duroquinone	blue LED	60	28
7	DMSO- <i>d</i> ₆	1,4-dinitrobenzene	blue LED	60	63
8	DMSO- <i>d</i> ₆	MV ²⁺	blue LED	36	88
9	DMSO- <i>d</i> ₆	none	blue LED	60	32
10	DMSO- <i>d</i> ₆	MV ²⁺	no light	60	0

^aConditions: 0.01 mol of Ir–Pt complex, 10.0 equiv of electron acceptor, room temperature. Irradiation was delivered at a distance of 5 cm away from the light source. ^bDetermined by ¹H NMR using 1,4-dimethoxybenzene as an internal standard. ^cDetermined by GC using mesitylene as an internal standard.

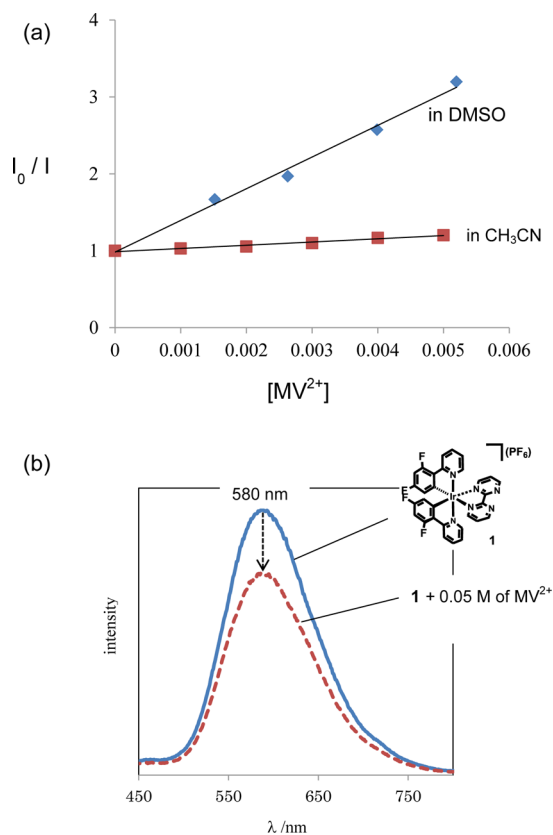


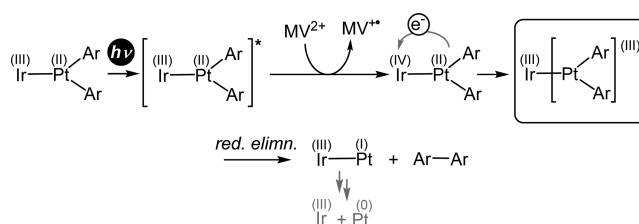
Figure 5. (a) Stern–Volmer studies of $[\text{Ir}(\text{dFppy})_2(\text{bpm})](\text{PF}_6)$ (**1**). Conditions: λ_{ex} 400 nm, λ_{obs} 580 nm. (b) Emission spectra for **1** (λ_{ex} 365 nm).

Ir center, we performed a luminescence quenching study, whose results are shown in Figure 5 (Stern–Volmer plot).³¹ As shown in the figure, the emission intensity decreases as the acceptor concentration ($[\text{MV}^{2+}]$) increases (Figure 4a). The ratio I_0/I (I_0 = emission intensity without acceptor, I = emission intensity with acceptor) is proportional to the acceptor concentration, which shows that MV^{2+} takes part in the photoredox quenching of the Ir(III)–cyclometalate unit through one-electron transfer. As the slope of the plot is larger in the DMSO solution, it supports the result that the reaction rate is much faster in DMSO than in CH_3CN (Table 4). The progress of electron transfer can be visually confirmed by the color change of the reaction solution from dark red to dark blue-green, which is due to the formation of a methylviologen radical cation ($\text{MV}^{+\bullet}$, dark blue) through one-electron reduction.

A plausible reaction mechanism of the visible-light-driven reductive elimination of the Ir–Pt complexes is presented in Scheme 2. Upon irradiation, the Ir(III)–Pt(II) complex is excited to $[\text{Ir}(\text{III})\text{–Pt}(\text{II})]^*$, which undergoes one-electron transfer to MV^{2+} to form the Ir(IV)–Pt(II) species. Formation of the Ir(IV)–Pt(II) species induces an intramolecular electron transfer from the Pt(II)–Ar₂ center to Ir(IV) to generate the Ir(III)–[Pt–Ar₂](III) species, resulting in the subsequent reductive elimination step to produce the biaryl product. Currently, we do not know the exact mechanism of the reaction that generates the Ir(III) complex **1** and Pt(0).

Photolysis of Ir–Pt Complexes in the Presence of Diphenyliodonium Salt. Next, we focused on the sacrificial electron acceptor as a radical source that needs to be used in the reductive elimination process. Diaryliodonium salts are often used as a radical source, since they generate aryl radicals

Scheme 2. Plausible Mechanism of Visible-Light-Driven Reductive Elimination



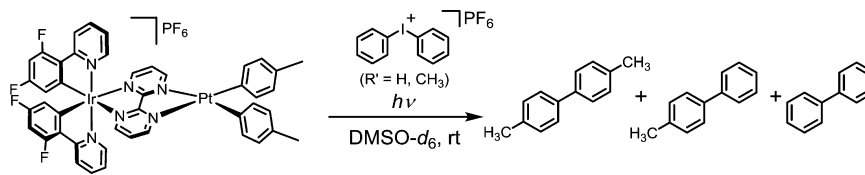
through one-electron reduction.³² Thus, diaryliodonium salts can act as both a sacrificial electron acceptor and an aryl radical source. To extend the quantitative reductive elimination of the reaction using the aryl radical, the photoreaction in the presence of a diaryliodonium salt was performed, and the results are summarized in Table 6. Irradiation of a DMF solution of Ir–Pt bis-tolyl complex **2b** with diphenyliodonium hexafluorophosphate generated 4,4′-dimethylbiphenyl (65%) together with 4-methylbiphenyl³³ (18%) and trace amounts of biphenyl (entry 1). When the irradiation was performed on the solution with a mixture of mononuclear Pt and Ir complexes, only trace amounts of 4-methylbiphenyl were formed with unidentified byproducts (entry 2). Thus, the dinuclear Ir–Pt motif is essential in the C–C bond-forming reductive elimination. Under the same conditions, when a solution of mononuclear Ir complex **1** was irradiated, the reaction did not take place at all (entry 3). Similarly, when either the diphenyliodonium salt (entry 4) or light (entry 5) was eliminated from the reaction conditions, only a trace amount of dimethylbiphenyl was formed. These results strongly suggest that the photoredox process of dinuclear Ir–Pt complexes with the diaryliodonium salt generates the aryl radical in the solution, which is involved in the reductive elimination to form the biaryls. When the reaction of **2a** with bis(4-methylphenyl)iodonium hexafluorophosphate was performed, similar amounts of biphenyl and 4-methylbiphenyl were formed (entry 6).

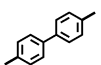
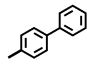
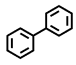
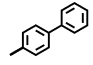
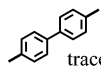
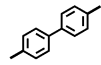
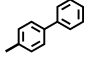
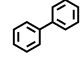
SUMMARY

We have synthesized a series of diarylplatinum complexes, which incorporated an Ir(III)–cyclometalate moiety as a photoredox site. The electrochemical and photophysical studies show that the photoredox-active Ir moiety can oxidize Pt(II)–Ar₂ to $[\text{Pt}\text{–Ar}_2](\text{III})$ via an intramolecular electron transfer. In the presence of a sacrificial electron acceptor, the Ir–Pt dinuclear complexes underwent *photoredox-mediated reductive elimination*, resulting in the quantitative formation of the corresponding biaryls at ambient temperature. Additionally, using a diphenyliodonium salt as both an electron acceptor and an aryl radical source, photoirradiation of the Ir–Pt complex afforded biaryls originating not only from the starting complex but also from the iodonium salt. The dinuclear motif was essential for these reactions. Our results indicate the possibility of molecular transformation by the combination of photoredox processes from metal complexes with various radical sources.

EXPERIMENTAL SECTION

General Procedures. Unless otherwise noted, all reactions were carried out under a nitrogen atmosphere. The solvents have been purified and dried according to standard methods. Methanol (Mg methoxide), CH_3NO_2 (CaCl_2), and DMSO (CaSO_4) were treated with the appropriate drying agents, distilled, and stored under N_2 . CH_2Cl_2 , Et_2O , and THF were purified through columns containing

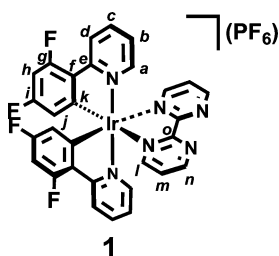
Table 6. Reductive Elimination of Biaryls in the Presence of Diaryliodonium Salt^a


Entry	Complex	Product ^b
1	2b	 65% +  18% +  trace
2 ^c	(bpy)Pt(<i>p</i> -tol) ₂ + 1	 + unidentified byproducts trace
3	1	N.D.
4 ^d	2b	 trace
5 ^e	2b	N.D.
6 ^f	2a	 6% +  32% +  34%

^aGeneral conditions: complex (0.01 mmol), diaryliodonium salt (0.012 mmol), in DMSO-*d*₆, irradiation with 3 W blue LED lamp (425 ± 15 nm) for 36 h. ^bProducts were determined by GC-MS. Yields were calculated on the basis of the mole ratio vs starting complex (**2a** or **2b**) using GC data. ^cIn CD₃CN. Undetermined byproducts were observed. ^dNo diaryliodonium salt. ^eNo light. ^fBis(4-methylphenyl)iodonium hexafluorophosphate ([I(*p*-tol)₂]PF₆) was used.

alumina and alumina–Cu catalyst and stored under a N₂ atmosphere. NMR solvents were dried over molecular sieves, degassed, and stored under N₂. Other chemicals were purchased and used as received. The ¹H NMR spectra were acquired on a Bruker AVANCE-400 (400 MHz) instrument. The NMR chemical shifts were referenced to residual proton signals in the deuterated solvent. UV–vis and emission spectra were obtained on JASCO V-670 and Hitachi F-7000 fluorescence spectrometers, respectively. Electrochemical measurements were recorded on a Hokutodenkou HZ-5000 analyzer (observed in CH₃CN; [(ⁿBu₄)BF₄] = 0.1 M; Ag/AgCl reference electrode; Pt working electrode; reported with respect to the [FeCp₂]/[FeCp₂]⁺ couple). Elemental analysis was performed with a LECO CHNS-932 VTF-900 instrument. Gas chromatography was carried out with a Shimadzu QP-5000 spectrometer. Single-crystal X-ray measurements were carried out on a Bruker SMART APEX II ULTRA diffractometer.

Preparation of **1**.

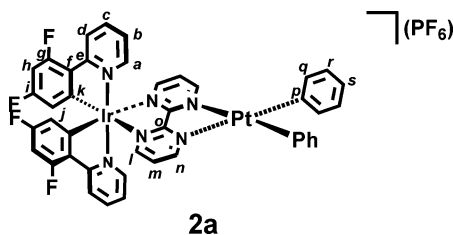


Under a nitrogen atmosphere, 2-(2,4-difluorophenyl)pyridine (dfppy; 3.10 g, 16.0 mmol) was added to a 2-ethoxyethanol/H₂O (160.0 mL, 3/1 v/v) solution of IrCl₃·3H₂O (2.82 g, 8.00 mmol). The reaction mixture was stirred at 110 °C for 24 h. After the mixture was cooled to room temperature, the precipitate was filtered and washed with H₂O and Et₂O. The residue was dried in vacuo to afford the Ir dimer [(dfppy)₂IrCl]₂ (4.20 g, 3.44 mmol, 86.1%). To a CH₂Cl₂/MeOH (180 mL, 2/1 v/v) solution of the Ir dimer (0.60 g, 0.49 mmol) was added 2,2'-bpm (0.20 g, 1.27 mmol), and the reaction mixture was stirred at 50 °C for 5 h. After the mixture was cooled to room temperature, KPF₆ (1.0 g) was added, the mixture was stirred for 4 h, and the solvent was evaporated under reduced pressure. The crude product was dissolved in CH₂Cl₂, and filtered through Celite to remove insoluble inorganic salts. The filtrate was evaporated, and the resulting solid was chromatographed on a silica gel with CH₂Cl₂/MeOH 95/5 (v/v) as eluent. The combined orange bands were evaporated. The solid was precipitated from CH₂Cl₂/Et₂O, washed with Et₂O and *n*-hexane several times, and then dried in vacuo to afford the title compound as a yellow powder (0.69 g, 0.79 mmol, 80%).

¹H NMR (400 MHz, CD₃NO₂, room temperature, δ/ppm) (signal assigned by ¹H–¹H COSY, HMQC, and HMBC): 9.20 (dd, *J* = 5.2 and 2.0 Hz, 2 H, H_n), 8.40 (dd, *J* = 5.2 and 2.0 Hz, 2 H, H_l), 8.35

(d, $J = 8.4$ Hz, 2 H, H_a), 7.94 (dd, $J = 8.4$ and 7.4 Hz, 2 H, H_b), 7.82 (d, $J = 6.0$ Hz, 2 H, H_d), 7.72 (dd, $J = 5.2$ and 5.2 Hz, 2 H, H_m), 7.11 (ddd, $J = 7.4, 6.0, 2.0$ Hz, 2 H, H_c), 6.68 (ddd, $J_{H-F} = 9.6, 9.2$ Hz, $^4J_{H-H} = 2.4$ Hz, 2 H, H_h), 5.82 (dd, $J_{H-F} = 9.2$ Hz, $^4J_{H-H} = 2.4$ Hz, 2 H, H_i). $^{13}\text{C}\{^1\text{H}\}$ NMR (100 MHz, CD_3NO_2 , room temperature, δ/ppm): 166.4, 164.3 (dd, $J_{\text{CF}} = 209.0, 13.0$ Hz, C_i), 165.2 (d, $J_{\text{CF}} = 7.0$ Hz, C_e), 163.8, 161.7 (dd, $J_{\text{CF}} = 203.0, 13.0$ Hz, C_g), 163.5 (C_o), 161.6 (C_l), 159.6 (C_n), 153.3 (d, $J_{\text{CF}} = 7.0$ Hz, C_f), 151.4 (C_d), 141.3 (C_b), 129.8 (C_k), 126.9 (C_m), 125.5 (C_c), 125.3 (C_a), 115.5 (d, $J_{\text{CF}} = 18.0$ Hz, C_j), 100.5 (t, $J_{\text{CF}} = 27.0$ Hz, C_h). ESI-MS: m/z 731 $[\text{M}(\text{PF}_6)]^+$. Anal. Calcd for $\text{C}_{30}\text{H}_{18}\text{N}_6\text{IrPF}_{10}$: C, 41.15; H, 2.07; N, 9.60. Found: C, 40.84; H, 2.07; N, 9.49.

Preparation of 2a.

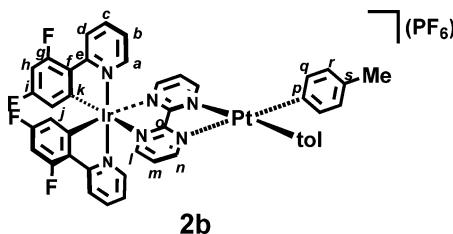


2a

In air, $[\text{Ir}(\text{dFppy})_2(\text{bpm})](\text{PF}_6)$ (288.6 mg, 0.33 mmol) and $(\text{DMSO})_2\text{PtPh}_2$ (202.2 mg, 0.40 mmol) were dissolved in CH_3CN (10 mL). The solution was stirred for 120 min at 55°C , and the solvent was removed under reduced pressure. The residue was washed with Et_2O and *n*-pentane several times and dried under vacuum. The product was obtained as a black solid (371.4 mg, 92%). Black crystals of $[\text{Ir}(\text{dFppy})_2(\text{bpm})\text{PtPh}_2](\text{PF}_6)$ suitable for crystallographic studies were grown by diffusing Et_2O vapors into a solution of the complex in CH_3CN .

^1H NMR (400 MHz, CD_3NO_2 , room temperature, δ/ppm) (signal assigned by $^1\text{H}-^1\text{H}$ COSY): 8.90 (dd, $J = 1.8, 5.5$ Hz, 2 H, H_n), 8.70 (dd, $J = 1.7, 5.5$ Hz, 2 H, H_i), 8.36 (d, $J = 8.4$ Hz, 2 H, H_a), 8.00–7.94 (m, 4 H, H_b, H_d), 7.86 (t, $J = 5.4$ Hz, 2 H, H_m), 7.34 (d, $J = 6.8$ Hz, 4 H, H_q), 7.16 (t, $J = 6.6$ Hz, 2 H, H_c), 6.96 (t, $J = 7.2$ Hz, 4H, H_l), 6.84 (t, $J = 7.2$ Hz, 2 H, H_s), 6.71 (ddd, $J = 2.0, 9.2, 12.0$ Hz, H_h), 5.82 (dd, $J = 2.2, 8.6$ Hz, 2H, H_j). ^{13}C NMR (400 MHz, CD_3NO_2 , room temperature, δ/ppm): 165.4 (C_o), 164.6, 162.5 (C_i), 163.3 (C_e), 162.0, 159.9 (C_g), 157.2 (C_l), 157.0 (C_n), 150.6 (C_d), 148.3 (C_f), 140.8 (C_p), 140.0 (C_b), 137.6 (C_q), 128.4 (C_m), 128.2 (C_k), 127.2 (C_r), 124.1 (C_a), 123.8 (C_c), 122.8 (C_s), 114.0 (C_j), 99.5 (C_h).

Preparation of 2b.



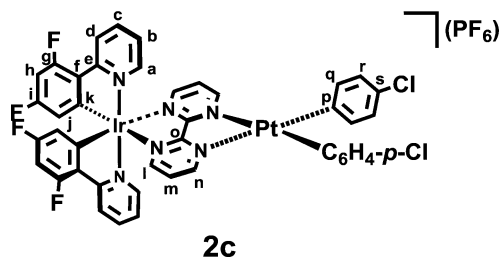
2b

In air, $[\text{Ir}(\text{dFppy})_2(\text{bpm})](\text{PF}_6)$ (68.4 mg, 0.078 mmol) and $(\text{DMSO})_2\text{Pt}(\text{tol})_2$ (50.0 mg, 0.094 mmol) were dissolved in CH_3CN (5 mL). The solution was stirred for 120 min at 55°C , and the solvent was removed under reduced pressure. The residue was washed with Et_2O and *n*-pentane several times and dried under vacuum. The product was obtained as a black solid (78.7 mg, 91%). Black crystals of $[\text{Ir}(\text{dFppy})_2(\text{bpm})\text{Pt}(\text{tol})_2](\text{PF}_6)$ suitable for crystallographic studies were grown by diffusing Et_2O vapors into a solution of the complex in CH_3CN .

^1H NMR (400 MHz, CD_3NO_2 , room temperature, δ/ppm) (signal assigned by $^1\text{H}-^1\text{H}$ COSY): 8.96 (dd, $J = 1.6$ and 5.6 Hz, 2 H, H_n), 8.71 (dd, $J = 1.6$ and 5.6 Hz, 2 H, H_i), 8.36 (d, $J = 8.4$ Hz, 2 H, H_a),

8.00–7.94 (m, 4 H, H_b and H_d), 7.86 (t, $J = 5.6$ Hz, 2 H, H_m), 7.27–7.10 (m, 6H, H_c and H_q), 6.80 (d, $J = 7.6$ Hz, 2 H, H_j), 6.71 (ddd, $J = 12.2, 9.6, 2.4$ Hz, 2 H, H_h), 5.82 (dd, $J = 8.8, 2.4$ Hz, 2 H, H_l), 2.17 (s, 6 H, Ar- CH_3). ^{13}C NMR (400 MHz, CD_3NO_2 , room temperature, δ/ppm): 167.1 (C_o), 166.3, 164.1 (C_i), 164.9 (C_e), 163.7, 161.5 (C_g), 158.7 (C_l), 158.6 (C_n), 152.2 (C_d), 150.0 (C_f), 141.7 (C_b), 139.0 (C_q), 138.2 (C_p), 133.5 (C_s), 130.2 (C_m), 129.9 (C_r), 129.7 (C_k), 125.6 (C_a), 125.4 (C_c), 115.6 (C_j), 101.1 (C_h), 21.1 (Ar- CH_3). Anal. Calcd for $\text{C}_{44}\text{H}_{32}\text{F}_{10}\text{IrN}_6\text{P}_2\text{Cl}_2$: C, 42.69; H, 2.73; N, 7.58. Found: C, 42.31; H, 2.87; N, 7.26.

Preparation of 2c.

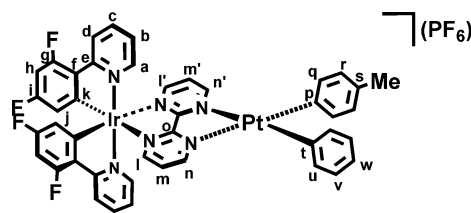


2c

In air, $[\text{Ir}(\text{dFppy})_2(\text{bpm})](\text{PF}_6)$ (68.4 mg, 0.080 mmol) and $(\text{DMSO})_2\text{Pt}(\text{C}_6\text{H}_4\text{-}p\text{-Cl})_2$ (50.0 mg, 0.095 mmol) were dissolved in CH_3CN (5 mL). The solution was stirred for 120 min at 55°C , and the solvent was removed under reduced pressure. The residue was washed with Et_2O and *n*-pentane several times and dried under vacuum. The product was obtained as a black solid (90 mg, 87%).

^1H NMR (400 MHz, CD_3NO_2 , room temperature, δ/ppm) (signal assigned by $^1\text{H}-^1\text{H}$ COSY): 8.86 (dd, $J = 1.6$ and 5.6 Hz, 2 H, H_n), 8.71 (dd, $J = 1.6$ and 5.6 Hz, 2 H, H_i), 8.37 (d, $J = 8.8$ Hz, 2 H, H_a), 7.98 (t, $J = 3.6$ Hz, 2 H, H_b), 7.95 (d, $J = 7.6$ Hz, 2 H, H_d), 7.87 (t, $J = 5.6$ Hz, 2 H, H_m), 7.32 (d, $J = 7.6$ Hz, 4 H, H_q), 7.20 (t, $J = 8.8$ Hz, 2 H, H_c), 6.99 (d, $J = 7.6$ Hz, 4 H, H_j), 6.71 (ddd, $J = 2.0, 9.2, 11.2$ Hz, 2 H, H_h), 5.81 (dd, $J = 2.0, 8.4$ Hz, 2 H, H_l). ^{13}C NMR (400 MHz, CD_3NO_2 , room temperature, δ/ppm): 167.0 (C_o), 166.4, 164.1 (C_i), 164.9 (C_e), 163.7, 161.7 (C_g), 159.1 (C_l), 158.7 (C_n), 152.2 (C_d), 149.8 (C_f), 141.8 (C_b), 140.3 (C_q), 130.2 (C_m), 130.0 (C_k), 129.8 (C_r), 125.7 (C_a), 125.5 (C_c), 115.6 (C_j), 101.2 (C_h). Anal. Calcd for $\text{C}_{42}\text{H}_{26}\text{Cl}_2\text{F}_{10}\text{IrN}_6\text{P}_2$: C, 38.99; H, 2.03; N, 6.50. Found: C, 38.49; H, 2.13; N, 6.58.

Preparation of 2d.



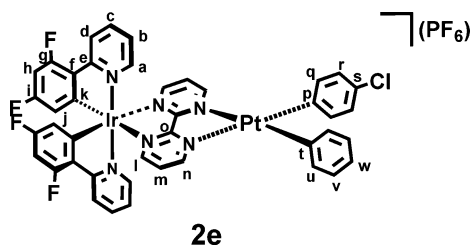
2d

In air, $[\text{Ir}(\text{dFppy})_2(\text{bpm})](\text{PF}_6)$ (152.5 mg, 0.17 mmol) and $(\text{DMSO})_2\text{PtPh}(\text{C}_6\text{H}_4\text{-}p\text{-Me})$ (108.6 mg, 0.21 mmol) were dissolved in CH_3CN (5 mL). The solution was stirred for 120 min at 55°C , and the solvent was removed under reduced pressure. The residue was washed with Et_2O and *n*-pentane several times and dried under vacuum. The product was obtained as a black solid (189.6 mg, 90%).

^1H NMR (400 MHz, CD_3NO_2 , room temperature, δ/ppm) (signal assigned by $^1\text{H}-^1\text{H}$ COSY): 8.970–8.893 (m, 2 H, H_n, H_i), 8.71 (ddd, $J = 0.8, 1.6, 5.6$ Hz, 2 H, H_l), 8.36 (d, $J = 8.8$ Hz, 2 H, H_d), 7.98 (t, $J = 7.6$ Hz, 2 H, H_b), 7.95 (d, $J = 5.6$ Hz, 2 H, H_j), 7.87–7.86 (m, 2 H, H_m), 7.33 (t, $J = 7.2$ Hz, 2 H, H_q), 7.21–7.14 (m, 4 H, H_c and H_a), 6.983–6.94 (m, 2 H, H_v), 6.85–6.79 (m, 2 H, H_u and H_w), 6.71 (ddd, $J = 2.4, 9.6, 12.4$ Hz, 2 H, H_h), 5.82 (dd, $J = 2.4$ and 8.8 Hz, 2 H, H_j), 2.17 (s, 3 H, Ar- CH_3). ^{13}C NMR (400 MHz, CD_3NO_2 , room

temperature, δ /ppm): 167.1 (C_o), 166.3, 163.8 (C_i), 164.9 (C_e), 163.7, 161.6 (C_g), 158.8 (C_l), 158.6 (C_n and C_n'), 152.3 (C_d), 150.1 (C_f), 141.7 (C_b), 139.2 (C_q), 139.0 (C_u), 130.0 (C_m), 129.8 (C_v), 129.7 (C_r), 125.7 (C_a), 125.6 (C_c), 125.4 (C_t or C_p), 124.4 (C_w), 115.5 (C_j), 101.1 (C_h), 21.5 (Ar-CH₃). Anal. Calcd for C₄₃H₃₀F₁₀IrN₆Pt + 0.7CH₂Cl₂: C, 40.25; H, 2.44; N, 6.43. Found: C, 40.10; H, 2.35; N, 6.93.

Preparation of 2e.



In air, [Ir(dFppy)₂(bpm)](PF₆) (98.5 mg, 0.011 mmol) and (DMSO)₂PtPh(C₆H₄-*p*-Cl) (72.9 mg, 0.013 mmol) were dissolved in CH₃CN (5 mL). The solution was stirred for 120 min at 55 °C, and the solvent was removed under reduced pressure. The residue was washed with Et₂O and *n*-pentane several times and dried under vacuum. The product was obtained as a black solid (126.7 mg, 89%).

¹H NMR (400 MHz, CD₃NO₂, room temperature, δ /ppm) (signal assigned by ¹H-¹H COSY): 8.88 (d, J = 5.2 Hz, 2H, H_n), 8.71 (d, J = 5.2 Hz, 2H, H_i), 8.36 (d, J = 8.4 Hz, 2H, H_a), 7.98 (t, J = 8.0 Hz, 2H, H_b), 7.93 (d, J = 5.6 Hz, 2H, H_d), 7.87 (t, J = 5.2 Hz, 2H, H_m), 7.36–7.31 (m, 4H, H_q and H_u), 7.16 (t, J = 6.8 Hz, 2H, H_c), 6.99–6.84 (m, 4H, H_r and H_v), 6.86 (t, J = 6.8 Hz, 1H, H_w), 6.71 (ddd, J = 2.0, 9.2, 12.0 Hz, 2H, H_h). ¹³C NMR (400 MHz, CD₃NO₂, room temperature, δ /ppm): 167.0 (C_o), 166.2, 164.1 (C_i), 163.6, 161.5 (C_g), 159.0 (C_l), 158.6 (C_n), 152.2 (C_d), 149.9 (C_f), 141.9 (C_e), 141.7 (C_k), 140.9 (C_s), 140.4 (C_q or C_u), 139.1 (C_q or C_u), 130.1 (C_m), 129.8 (C_r), 129.0 (C_v or C_v), 128.5 (C_r or C_v), 125.7 (C_a), 125.6 (C_c), 124.6 (C_w), 115.5 (C_j), 101.1 (C_h). Anal. Calcd for C₄₂H₂₇ClF₁₀IrN₆Pt + 0.5 CH₃CN: C, 40.35; H, 2.24; N, 7.11. Found: C, 40.45; H, 2.24; N, 7.35.

General Procedure for Visible-Light-Mediated Reductive Elimination of Biaryl from 2. Irradiation of visible light was performed with a Somakogaku xenon lamp (150 W) or a Relyon LED lamp (3 W × 2; λ 425 nm). The Ir–Pt complex (0.01 mmol), MV²⁺ (47.6 mg, 0.10 mmol), and 1,4-dimethoxybenzene (2.0 mg as an internal standard) were dissolved in DMSO-*d*₆ (0.45 mL) in a 5 mm i.d. NMR tube. The reaction mixture was degassed by a freeze–pump–thaw cycle. The reaction was carried out at room temperature (water bath) under visible-light irradiation (placed at a distance of 5 cm from the light source). Biaryl products formed in the reaction were determined by ¹H NMR and GCMS spectra.

Crystal Structure Determination. The crystallographic data and the results of the structure refinements are summarized in Table S1 in the Supporting Information. Lorentz and polarization corrections and empirical absorption corrections were made during the data reduction.³⁴ The structures were solved by a combination of direct methods (SHELXS-86)³⁵ and Fourier synthesis (DIRDIF94).³⁶ Unless otherwise stated, all non-H atoms were refined anisotropically, and all H atoms were fixed at the calculated positions.

■ ASSOCIATED CONTENT

Supporting Information

Tables, figures, and a CIF file giving crystal data, bond distances, and bond angles for **1** and **2a,b**, optimized geometries of **2a–c** and **2a⁺**, frontier orbitals of **2a–c**, NMR spectra, and GCMS data of the reductive elimination reactions. The Supporting Information is available free of charge on the ACS Publications website at DOI: 10.1021/om501080v.

■ AUTHOR INFORMATION

Corresponding Authors

*E-mail for A.I.: ainagaki@tmu.ac.jp.

*E-mail for M.A.: makita@res.titech.ac.jp.

Notes

The authors declare no competing financial interest.

■ ACKNOWLEDGMENTS

This research was financially supported by JSPS KAKENHI (C) Grant Number 24550071, the Cooperative Research Program of “Network Joint Research Center for Materials and Devices”, Naito Foundation Subsidy for Female Researchers, and Tokyo Ohka Foundation for the Promotion of Science and Technology; this support is gratefully acknowledged. A part of this work was supported by a JSPS Grant-in-Aid for Scientific Research on Innovative Areas “3D Active-Site Science”: Grant No. 26105003.

■ REFERENCES

- (1) Neufeldt, S. R.; Sanford, M. S. *Acc. Chem. Res.* **2012**, *45*, 936.
- (b) Beck, E. M.; Gaunt, M. J. *Top. Curr. Chem.* **2010**, *292*, 85. (c) Ren, Z.; Mo, F.; Dong, G. *J. Am. Chem. Soc.* **2012**, *134*, 16991. (d) Ding, S.-T.; Jiao, N. *J. Am. Chem. Soc.* **2011**, *133*, 12374–12377. (e) Ye, M.; Gao, G.-L.; Yu, J.-Q. *J. Am. Chem. Soc.* **2011**, *133*, 6964. (f) Chen, M. S.; Prabakaran, N.; Labenz, N. A.; White, M. C. *J. Am. Chem. Soc.* **2005**, *127*, 6970. (g) Dick, A. R.; Hull, K. L.; Sanford, M. S. *J. Am. Chem. Soc.* **2004**, *126*, 2300.
- (a) McKeown, B. A.; Foley, M. A.; Lee, J. P.; Gunnoe, T. B. *Organometallics* **2008**, *27*, 4031. (b) McKeown, B. A.; Gonzalez, H. E.; Friedfeld, M. R.; Gunnoe, T. B.; Cundari, T. R.; Sabat, M. *J. Am. Chem. Soc.* **2011**, *133*, 19131.
- (a) Gol'dshleger, N. F.; Tyabin, M. B.; Shilov, A. E.; Shteinman, A. A. *Zh. Fiz. Khim.* **1972**, *46*, 785. (b) Periana, Roy A.; Taube, D. J.; Gamble, S.; Taube, H.; Satoh, T.; Fujii, H. *ChemInform* **1998**, DOI: 10.1002/chin.199829357.
- (4) Kurosawa, H.; Yamamoto, A. *Fundamentals of Molecular Catalysis*; Elsevier: New York, 2003, Vol. 3, p 479.
- (5) Marcone, J. E.; Moloy, K. G. *J. Am. Chem. Soc.* **1998**, *120*, 8527.
- (a) Korenaga, T.; Abe, K.; Ko, A.; Maenishi, R.; Sakai, T. *Organometallics* **2010**, *29*, 4025. (b) Shekhar, S.; Hartwig, J. F. *J. Am. Chem. Soc.* **2004**, *126*, 13016. (c) Merwin, R. K.; Schnabel, R. C.; Koola, J. D.; Roddick, D. M. *Organometallics* **1992**, *11*, 2972.
- (7) Hartwig, J. F. *Inorg. Chem.* **2007**, *46*, 1936.
- (8) Liberman-Martin, A. L.; Bergman, R. G.; Tilley, T. D. *J. Am. Chem. Soc.* **2013**, *135*, 9612.
- (9) The Komiya group has reported visible-light-driven reductive elimination from a Pt–Mn dinuclear complex: Komiya, S.; Ezumi, S.; Komine, N.; Hirano, M. *Organometallics* **2009**, *28*, 3608.
- (10) Juris, A.; Barigelletti, V.; Campagna, F.; S. Belsler, P.; von Zelewsky, A. *Coord. Chem. Rev.* **1988**, *84*, 85.
- (11) Flamigni, L.; Barbieri, A.; Sabatini, C.; Ventura, B.; Barigelletti, F. *Top. Curr. Chem.* **2007**, *281*, 143.
- (12) (a) Slinker, J. D.; Gorodetsky, A. A.; Lowry, M. S.; Wang, J.; Parker, S.; Rohl, R.; Bernhard, S.; Malliaras, F. G. *J. Am. Chem. Soc.* **2004**, *126*, 2763. (b) Lowry, M. S.; Goldsmith, J. I.; Slinker, J. D.; Rohl, R.; Pascal, R. A., Jr.; Malliaras, G. G.; Bernhard, S. *Schem. Mater.* **2005**, *17*, 5712. (c) Hanss, D.; Freys, J. C.; Bernardinelli, G.; Wenger, O. S. *Eur. J. Inorg. Chem.* **2009**, *2009*, 4850.
- (13) (a) Zuo, Z.; Ahneman, D. T.; Chu, L.; Terrett, J. A.; Doyle, A. G.; MacMillan, D. W. C. *Science* **2014**, *345*, 437. (b) Noble, A.; MacMillan, D. W. C. *J. Am. Chem. Soc.* **2014**, *136*, 11602. (c) Prier, C. K.; Rankic, D. A.; MacMillan, D. W. C. *Chem. Rev.* **2013**, *113*, 5322. (d) Yasu, Y.; Koike, T.; Akita, M. *Chem. Commun.* **2012**, *48*, 5355. (e) Yasu, Y.; Koike, T.; Akita, M. *Angew. Chem., Int. Ed.* **2012**, *51*, 9567. (f) Koike, T.; Yasu, Y.; Akita, M. *Chem. Lett.* **2012**, *41*, 999. (g) Yasu, Y.; Koike, T.; Akita, M. *Adv. Synth. Catal.* **2012**, *354*, 3414.

- (14) (a) Murata, K.; Inagaki, A.; Akita, M.; Halet, J.-F.; Costuas, K. *Inorg. Chem.* **2013**, *52*, 8030. (b) Nitadori, H.; Takahashi, T.; Inagaki, A.; Akita, M. *Inorg. Chem.* **2012**, *51*, 51. (c) Inagaki, A.; Nakagawa, H.; Akita, M.; Inoue, K.; Sakai, M.; Fujii, M. *Dalton Trans.* **2008**, 6709. (d) Inagaki, A.; Yatsuda, S.; Edure, S.; Suzuki, A.; Takahashi, T.; Akita, M. *Inorg. Chem.* **2007**, *46*, 2432. (e) Inagaki, A.; Edure, S.; Yatsuda, S.; Akita, M. *Chem. Commun.* **2005**, 5468. (f) Saita, T.; Nitadori, H.; Inagaki, A.; Akita, M. *J. Organomet. Chem.* **2009**, *694*, 3125. (g) Murata, K.; Araki, M.; Inagaki, A.; Akita, M. *Dalton Trans.* **2013**, *42*, 6989. (h) Murata, K.; Ito, M.; Inagaki, A.; Akita, M. *Chem. Lett.* **2010**, 39, 915.
- (15) (a) Kozawa, K.; Inagaki, A.; Akita, M. *Chem. Lett.* **2014**, *43*, 290.
- (16) By detecting emission attenuation, the emission lifetime was 80 ns in degassed acetonitrile solution, with 355 nm excitation by YAG laser pulse. The emission intensity of the ppy (2-phenylpyridine) counterpart was too weak (probably due to short lifetime) to be detected.
- (17) (a) Chaudhury, N.; Puddephat, R. J. *J. Organomet. Chem.* **1975**, *84*, 105. (b) Lanza, S.; Minniti, D.; Moore, P.; Sachinidis, J.; Romeo, R.; Tobe, M. L. *Inorg. Chem.* **1984**, *23*, 4428.
- (18) Peters, T. B.; Zheng, Q.; Stahl, J.; Bohling, J. C.; Arif, A. M.; Hampel, F.; Gladysz, J. A. *J. Organomet. Chem.* **2002**, *641*, 53.
- (19) (a) Aoki, S.; Matsuo, Y.; Ogura, S.; Ohwada, H.; Hisamatsu, Y.; Moromizato, S.; Shiro, M.; Kitamura, M. *Inorg. Chem.* **2011**, *50*, 806. (b) Yi, C.; Yang, C.-J.; Liu, J.; Xu, M.; Wang, J.-H.; Cao, Q.-Y.; Gao, X.-C. *Inorg. Chim. Acta* **2007**, *360*, 3493.
- (20) Complex **1** has been preliminarily analyzed, and the data are given in the Supporting Information.
- (21) Klein, A.; Hausen, H.-D.; Kaim, W. *J. Organomet. Chem.* **1992**, *440*, 207.
- (22) Calvert, J. M.; Caspar, J. V.; Binstead, R. A.; Westmoreland, T. D.; Meyer, T. J. *J. Am. Chem. Soc.* **1982**, *104*, 6620.
- (23) Costa, R. D.; Ortí, E.; Bolink, H. J.; Monti, F.; Accorsi, G.; Armaroli, N. *Angew. Chem., Int. Ed.* **2012**, *51*, 8178.
- (24) Klein, A.; Van Slageren, J.; Zális, S. *Eur. J. Inorg. Chem.* **2003**, 2003, 1917.
- (25) Didier, P.; Ortmans, I.; Mesmaeker, A. K.-D.; Watts, R. J. *Inorg. Chem.* **1993**, *32*, 5239.
- (26) Serroni, S.; Juris, A.; Campagna, S.; Venturi, M.; Denti, G.; Balzani, V. *J. Am. Chem. Soc.* **1994**, *116*, 9086.
- (27) (a) Usón, R.; Forniés, J.; Tomás, M.; Menjón, B.; Bau, R.; Stükel, K.; Kuwabara, E. *Organometallics* **1986**, *5*, 1576. (b) Rieger, A. L.; Carpenter, G. B.; Rieger, P. H. *Organometallics* **1993**, *12*, 842. (c) Bond, A. M.; Colton, R.; Fieldler, D. A.; Kevekordes, J. E.; Tedesco, V. *Inorg. Chem.* **1994**, *33*, 5761. (d) Klein, A.; Kaim, W. *Organometallics* **1995**, *14*, 1176.
- (28) Vogler, C.; Schwederski, B.; Klein, A.; Kaim, W. *J. Organomet. Chem.* **1992**, *436*, 367.
- (29) Frisch, M. J.; Trucks, G. W.; Schlegel, H. B.; Scuseria, G. E.; Robb, M. A.; Cheeseman, J. R.; Scalmani, G.; Barone, V.; Mennucci, B.; Petersson, G. A.; Nakatsuji, H.; Caricato, M.; Li, X.; Hratchian, H. P.; Izmaylov, A. F.; Bloino, J.; Zheng, G.; Sonnenberg, J. L.; Hada, M.; Ehara, M.; Toyota, K.; Fukuda, R.; Hasegawa, J.; Ishida, M.; Nakajima, T.; Honda, Y.; Kitao, O.; Nakai, H.; Vreven, T.; Montgomery, J. A., Jr.; Peralta, J. E.; Ogliaro, F.; Bearpark, M.; Heyd, J. J.; Brothers, E.; Kudin, K. N.; Staroverov, V. N.; Keith, T.; Kobayashi, R.; Normand, J.; Raghavachari, K.; Rendell, A.; Burant, J. C.; Iyengar, S. S.; Tomasi, J.; Cossi, M.; Rega, N.; Millam, J. M.; Klene, M.; Knox, J. E.; Cross, J. B.; Bakken, V.; Adamo, C.; Jaramillo, J.; Gomperts, R.; Stratmann, R. E.; Yazyev, O.; Austin, A. J.; Cammi, R.; Pomelli, C.; Ochterski, J. W.; Martin, R. L.; Morokuma, K.; Zakrzewski, V. G.; Voth, G. A.; Salvador, P.; Dannenberg, J. J.; Dapprich, S.; Daniels, A. D.; Farkas, O.; Foresman, J. B.; Ortiz, J. V.; Cioslowski, J.; Fox, D. J. *Gaussian 09, Revision D.01*; Gaussian, Inc.: Wallingford CT, 2013.
- (30) See the Supporting Information for detailed calculation results.
- (31) Since dinuclear Ir–Pt complexes show very weak emission, the mononuclear Ir complex is used for this study.
- (32) (a) Kalyani, D.; McMurtrey, K. B.; Neufeldt, S. R.; Sanford, M. S. *J. Am. Chem. Soc.* **2011**, *133*, 18566. (b) Neufeldt, S. R.; Sanford, M. S. *Adv. Synth. Catal.* **2012**, *354*, 3517.
- (33) Confirmed by ¹H NMR and GC-MS (Figure S3, Supporting Information) spectra.
- (34) Higashi, T. *Program for absorption correction*; Rigaku Corp., Tokyo, Japan, 1995.
- (35) (a) Sheldrick, G. M. *SHELXS-86: Program for crystal structure determination*; University of Göttingen, Göttingen, Germany, 1986. (b) Sheldrick, G. M. *SHELXL-97: Program for crystal structure refinement*, University of Göttingen, Göttingen, Germany, 1997.
- (36) DIRDIF99: Beurskens, P. T.; Admiraal, G.; Beurskens, G.; Bosman, W. P.; de Gelder, R.; Israel, R.; Smits, J. M. M. *The DIRDIF-99 program system*; Technical Report of the Crystallography Laboratory; University of Nijmegen, Nijmegen, The Netherlands, 1999.